Noncollinear gating for high-flux isolated-attosecond-pulse generation

Shiyang Zhong, Xinkui He,* Yujiao Jiang, Hao Teng, Peng He, Yangyang Liu, Kun Zhao, and Zhiyi Wei†
Beijing National Laboratory for Condensed Matter Physics, Institute of Physics, Chinese Academy of Sciences, Beijing 100190, China
(Received 26 November 2015; published 29 March 2016)

We propose an approach for producing high-flux isolated-attosecond pulses (IAPs) based on noncollinear geometry of high-order harmonic generation (HHG). By combining a main driving pulse and an ultrashort gating pulse in the interaction medium to form a tilt wave front in a very narrow overlapping time region, the attosecond pulses generated in this region are spatially separated from the original beam in the far field. It gives a way of extracting IAPs as well as fully characterizing an attosecond-pulse train (APT). Since this approach set no restriction on the pulse duration of the main driving pulse, it is particularly suitable for high-flux IAP generation by a high-energy laser which usually has multicycle pulse duration.

DOI: 10.1103/PhysRevA.93.033854

I. INTRODUCTION

Attosecond physics has enhanced our understanding of the ultrafast electron dynamics in atoms, molecules, and condensed matters with its unprecedented temporal resolution since the first demonstration of isolated-attosecond-pulse (IAP) generation in 2001 [1]. A lot of significant progress has been made during the first decade of this new research field, such as attosecond streaking [2], tunneling and recollision spectroscopy [3], molecular orbit tomography [4], and controlling and probing dielectric properties [5,6].

However, the complete observation and manipulation of ultrafast phenomena requires a true attosecond-pump and attosecond-probe scheme which is currently very challenging due to the limited flux of the IAP [7]. At present, up to tens of microjoule high-energy attosecond-pulse train (APT) generation has been reported applying the loosely focusing geometry [8] which is sufficient for nonlinear attosecond physics, but the generation of intense IAP remains to be tough work, though advances have been made in recent years [9,10]. There are naturally two routes to improve the output flux of IAP: improving the high harmonic conversion efficiency and using high-energy driving lasers. The improvement of conversion efficiency has been investigated in both single-atom and macroscopic scales. An efficiency of 10^{-4} level has been achieved [9]. On the other hand, the conventional gating techniques for IAP generation such as amplitude gating [11], polarization gating [12], and ionization gating [13] usually require a sub-5 fs driving laser pulse, which prevents the use of high-energy driving lasers with pulse duration typically longer than 30 fs. Generalized double optical gating (GDOG) [14,15] enables a relaxation on the driving pulse duration requirements up to 30 fs. However, the relatively short pulse duration still remains a key factor for reducing the ionization before the arrival of the linear polarized gate, which is critical for a good single-atom conversion efficiency [10]. Attosecond lighthouse [16,17] based on wave front rotation (WFR) of the driving pulses have been demonstrated to generate angularly separated IAPs with simple implementation and relatively long driving laser pulses, but maximum duration limit is still necessary to ensure the spatial separation of attosecond pulses from subsequent half-optical cycles. Recently, noncollinear optical gating (NOG) [18,19] has been demonstrated based on noncollinear geometry and WFR technique for IAP generation. Two identical pulses noncollinearly overlap with specific temporal delay to form a rotated wave front for separating IAP in the far field. The duration limit still remains, similar to the attosecond lighthouse. Only the overlapped edge of the two pulses can be used which limits the intensity and photoenergy of the IAP. In these conventional IAP generation methods, the driving pulse takes the responsibility for both attosecond-pulse generation and the single pulse extraction. If the two tasks for the driving laser pulse can be separated and taken by two different pulses respectively, then the constraint on the driving pulse may be completely released and a high-energy laser can be used.

II. ANALYTICAL MODEL

In this paper we propose a scheme for generating high-flux IAP, aiming at eliminating the driving pulse duration limitation in IAP generation. Enlightened by the concept of WFR, the scheme is based on the noncollinear geometry of HHG. Noncollinear HHG provides natural separation of HHG from a fundamental beam ideal for IAP selection. The spatial separation of noncollinear HHG has been studied [20] and employed for space-time measurements of attosecond pulses [21], as well as the NOG technique mentioned above. The scheme combines a main driving pulse regardless of pulse duration for generating APT and a subcycle gating pulse for exacting an IAP from the pulse train. The principle of the scheme is illustrated in Fig. 1. The two pulses are noncollinearly overlapped at the focus point and interact with the medium. The isolated-attosecond pulse can be spatially extracted when the duration of the gating pulse is short enough and the laser wave front within only one half-cycle is tilted. By completely releasing the constraint for the driving pulse, the scheme is especially suited for IAP generation using a long and intense laser pulse. The rigorous demand on driving pulse duration is now transferred to the gating pulse, which serves as a perturbation to the generation process and can be much weaker.

Our approach is based on the WFR induced by the temporal overlapping of two noncollinear driving pulses. As indicated

*xinkuihe@iphy.ac.cn
†zywei@iphy.ac.cn

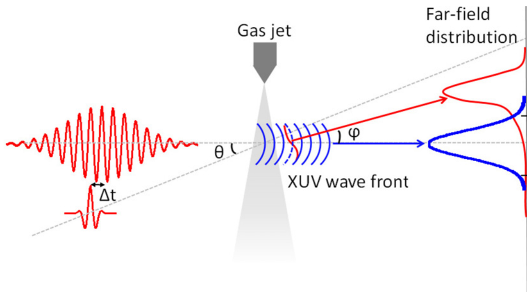

FIG. 1. Principle illustration of the scheme of the IAP generation. A long driving pulse and a short gating pulse with a noncollinear angle θ and time delay Δt overlap in the gas medium. The distorted XUV wave front induced by the gating pulse in the overlapping region lead to off-axis IAP with a propagation angle φ.

in Fig. 1, the wave vector $\vec{k}$ of the synthesized field is inside the angle sector of the two driving field $\vec{k}_1$ and $\vec{k}_2$. The instantaneous total wave vector is expressed as [18]

$$\vec{k} = \frac{\vec{k}_1 + \xi \vec{k}_2}{\sqrt{1+\xi^2}}, \tag{1}$$

where ξ is the ratio of the field envelope of the two driving field $\varepsilon_2/\varepsilon_1$. Assuming both pulses have Gaussian temporal profile, $\varepsilon_1 = E_1 \exp[-2\ln(2)(t)^2/\tau_1^2]$ and $\varepsilon_2 = E_2 \exp[-2\ln(2)(t-\Delta t)^2/\tau_2^2]$, where E and τ denote the amplitude and pulse duration of the driving field, and Δt denotes the time delay. Since the propagation direction of the high-order harmonics follows the wave vector of the driving field, we can expect the attosecond pulses deflected from either direction of two driving beams. The time-dependent wave vector $\vec{k}(t)$ transfers to the spatial separation of the attosecond pulses in the far field. For small noncollinear angle θ, the time-dependent deflection angle of the attosecond pulses can be estimated as

$$\varphi(t) = \frac{\theta \xi(t)}{1+\xi(t)}. \tag{2}$$

Both attosecond lighthouse and NOG introduce such field distortion to several subsequent half-cycles and acquire several IAPs with different propagation angles in the far field. These methods impose restrictions on the upper limit of the driving pulse duration as a longer pulse can hardly afford sufficient WFR to fulfill far-field separation [16,18]. In our scheme, the secondary gating pulse is set to be short enough to confine the field distortion to a few half-cycles (ideally, only one half-cycle) of the main pulse. The selected half-cycle leads to off-axis IAP while the rest of the APT remains on-axis, available for further application, as shown in Fig. 1. The key parameter of this scheme is the pulse duration of the short gating pulse. The maximum gating pulse duration is defined by the condition when the angular separation of the attosecond pulses from subsequent half-cycles exceeds their angular divergence δ [22],

$$\varphi(t) - \varphi\left(t \pm \frac{T}{2}\right) \geqslant \delta, \tag{3}$$

$$\delta = \frac{\lambda_h}{\pi w_h}\sqrt{1 + 4\alpha_j^2 I_0^2 \frac{w_h^4}{w_f^4}}, \tag{4}$$

where T is the optical cycle of the main driving pulse. λ_h and ω_h are the wavelength and beam waist of the harmonics, I_0 and w_f are the peak power density and beam waist of the driving field, and α denotes the intensity dependence of the dipole phase [23]. The positive correlation of the deflection angle φ and envelope ratio (not intensity ratio) ξ implies a minimum requirement on the intensity of the gating pulse. According to Eqs. (2) and (3), the ratio of the two involving fields requires to be $\xi_0 = E_2/E_1 \geqslant \delta/(\theta - \delta)$, usually no less than 0.1. The time gate formatted by the gating pulse is denoted by the white dashed lines in Figs. 2(b) and 3(a). It has a width of $\tau_g = \sqrt{2\log_2(2+\xi_0)}\tau_2 \sim 1.5\tau_2$ when $\tau_2 \ll \tau_1$. On the other hand, at a certain adequate ratio ξ_0 and in case $E_2 \ll E_1$ and $\tau_2 \ll \tau_1$, the maximum gating pulse duration to separate subsequent attosecond pulses can be approximated from Eqs. (2) and (3),

$$\tau_2 \leqslant \frac{T}{2}\sqrt{\frac{2\ln(2)}{\ln(\varphi_0) - \ln(\varphi_0 - \delta)}}, \tag{5}$$

where $\varphi_0 = \theta\xi_0/(1+\xi_0)$ denotes maximum deflection angle. The estimation given in Eq. (5) indicates that the gating pulse duration is required to be in the scale of $T/2$. Considering typical experimental parameters $I_1 = 2 \times 10^{14}$ W/cm^2, $\tau_1 = 30$ fs, $\omega_f = 100$ μm, and $\theta = 10$ mrad, the divergence δ is estimated as 1.5 mrad at $1/e^2$ width for high orders of short trajectory. When $I_2 = 0.2 \times 10^{14}$ W/cm^2, corresponding to $\xi = 0.32$, the maximum rotation angle at is $\varphi_0 = 2.4$ mrad and the gating pulse is expected to be shorter than 1.6 fs. The generation of such a subcycle pulse is challenging, but already demonstrated by waveform synthesizing [24].

Despite its technical difficulties, IAP extraction using a short gating pulse has specific advantages. The gating pulse perturbs the generation process only in a small fraction of the main pulse. The IAP is changed little after selection and the APT from the rest of the main pulse remains unchanged. Any pulse in the APT can be extracted by simply changing the time delay of the two pulses. The spectrum, relative intensity, and pulse duration for each pulse in the train can thus be measured respectively, while the reconstruction of attosecond beating by interference of the two-photon transition (RABITT) method that is typically used in APT characterization only provides average temporal profile of the whole pulse train [25]. The flexibility of selecting an arbitrary pulse is significant to ensure the selection of the highest flux IAP since the peak of HHG does not always coincide with that of the driving laser pulse due to the ground state depletion and the propagation effect. The concept of the scheme is similar to a pump-probe process where the long intense main pulse acts as the pump and the short gating pulse acts as the time-delayed probe. Therefore, the scheme is potentially an *in situ* measurement of the HHG process as demonstrated in [21].

III. NUMERICAL RESULTS

The numerical simulation is performed to check the noncollinear gating technique we proposed above. The single atom response is calculated by solving a time-dependent Schrödinger equation in strong field approximation [26] along one dimension in the radial direction and only short trajectory contribution is considered. The far-field distribution at a

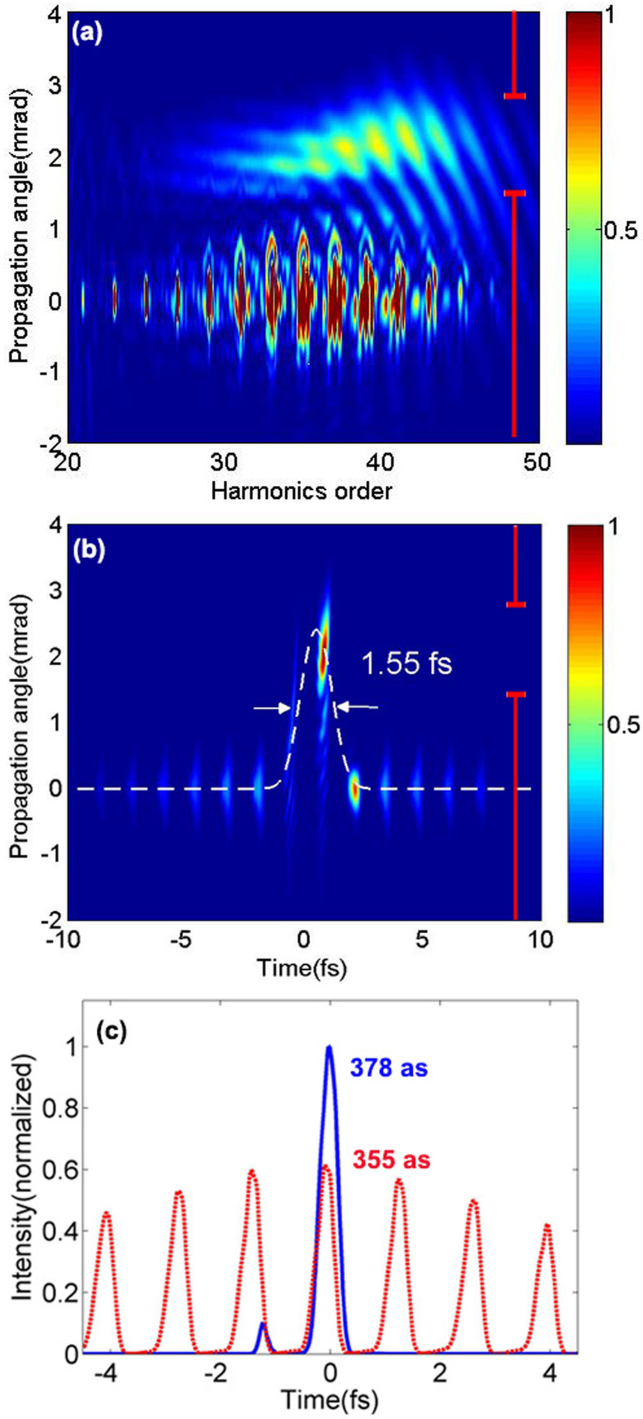

FIG. 2. The simulation results for the noncollinear IAP gating technique. The fundamental pulse $\tau_1 = 30$ fs at $\lambda_1 = 800$ nm with power density $I_1 = 2 \times 10^{14}$ W/cm^2, and the gating pulse $\tau_2 = 1$ fs, $I_2 = 0.2 \times 10^{14}$ W/cm^2, cross angle $\theta = 10$ mrad, time delay $\Delta t = 0.6$ fs. (a) The angular-resolved far-field spectrum of the on-axis APT and off-axis IAP. (b) Spatio-temporal distribution in the far field. The white dashed line indicates the gate width. (c) Blue line: IAP selected from the off-axis propagation angle between 1.5 and 3 mrad in the far field [as labeled by the red bar in (a) and (b)]. Doted red line: The corresponding attosecond pulse from APT without the gating pulse.

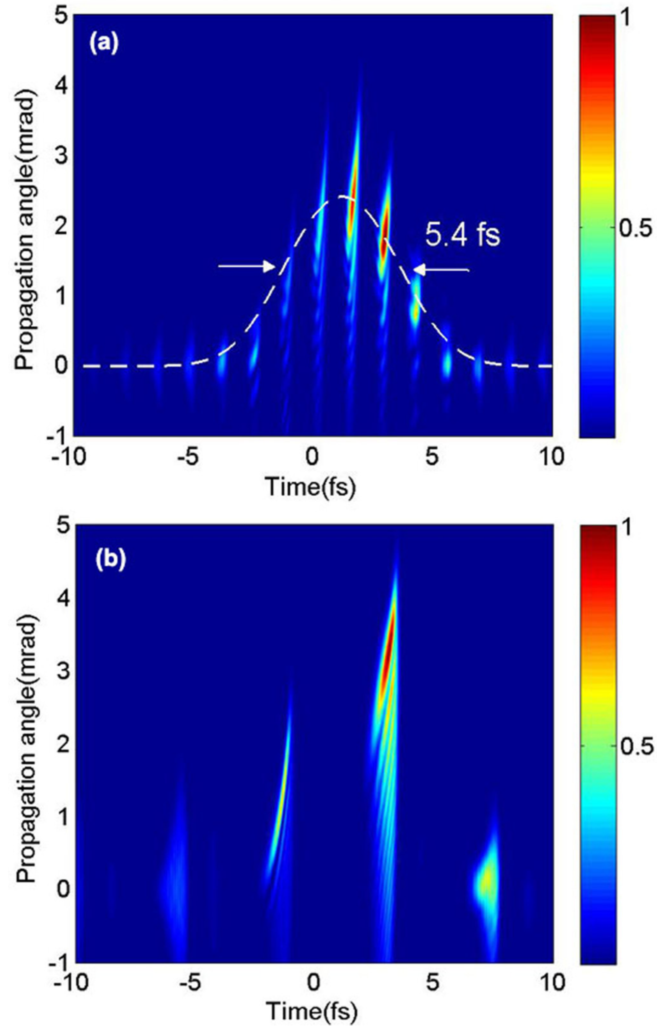

FIG. 3. The far-field HHG spatio-temporal distribution generated by (a) the same parameter in Fig. 2 except that gating pulse duration $\tau_2 = 3.5$ fs (corresponds to gate width 5.4 fs as the dashed line shows). (b) The fundamental pulse $\tau_1 = 30$ fs at $\lambda_1 = 1300$ nm with power density $I_1 = 1 \times 10^{14}$ W/cm^2, the gating pulse $\tau_2 = 3.5$ fs, $I_2 = 0.1 \times 10^{14}$ W/cm^2, and the second harmonics of the fundamental beam $I_3 = 0.1 \times 10^{14}$ W/cm^2, cross angle $\theta = 10$ mrad, time delay $\Delta t = 2.8$ fs.

distance of 1 m is calculated using Huygens integral in Fresnel approximation. The propagation effect is not taken into account.

The simulation result for HHG in neon is presented in Fig. 2. The spatial distribution of the high harmonic spectrum in the far field is shown in Fig. 2(a). The HHG from only one half-cycle is selected due to the ultrashort gating pulse. This off-axis continuum corresponds to a single attosecond burst. The spatio-temporal distribution of the far-field attosecond pulses in Fig. 2(b) fits well with the gate width (dashed line) calculated from Eq. (2). The coincidence verifies the validity of the simple analytical model given above. The gate width provided by the 1 fs gating pulse is estimated as 1.55 fs, coincident to the $T/2$ time scale of a single half-cycle. Figure 2(d) indicates the temporal profile of the off-axis IAP selected from far field, while the dashed line indicates the corresponding pulse from the APT without the gating pulse. The total intensity of the selected IAP is enhanced by the gating pulse, and the pulse duration is also slightly changed (from 355 to 378 as). Another interesting issue is the spatial chirp of the selected IAP in the far field. For a certain delay, the radiation generated at different time corresponds to different gating pulse intensity which leads to different propagation angles. The intrinsic temporal dispersion of the attosecond pulse is thus mapped into the spatial chirp in the far field. A shorter gating pulse with steeper slope in the intensity profile results in a stronger spatial chirp. In the noncollinear scheme, an off-axis geometrical mismatching term due to the gating pulse is added to the total wave-vector mismatch [27]. The additional mismatch can be compensated by the collinear term or by adjusting the experimental parameters. Thus the single atom response by a wave front rotated driving pulse is expected to survive in the macroscopic scale without inevitable decline in the harmonic conversion efficiency under adequate conditions. The contribution from long trajectories is also expected to be suppressed in the propagation effect by properly adjusting the gas jet position because the relatively large far-field divergence angle of long trajectory demands a much stricter parameter on the gating pulse.

As mentioned above, the main restriction of our scheme is the gating pulse duration. In the estimation and simulation results given above, the gating pulse is down to 1 fs which is technically challenging and limits the experimental accessibility. The far-field spatio-temporal distribution of the HHG with a 3.5 fs gating pulse which provides a 5.4 fs temporal gate is shown in Fig. 3(a). A longer gating pulse results in the APT off-axis in the far field. Several approaches can be used to relax the requirement of a gating pulse. Increasing the cross angle is the most straightforward method for better spatial separation, in others words a more relaxed gating requirement. However, the interference of the two driving fields leads to the multiple sources radiation at a larger cross angle. The multiple sources interference results in complicated spatial distribution of the selected IAP in the far field, which is unwanted for normal pump and probe experiments. Therefore, the noncollinear angle must be limited to a proper region to minimize the interference effect [17]. Another approach is to increase the ratio ξ of the two fields, relaxing the gating pulse duration at the cost of limiting the main pulse and gradually changing the perturbative role of the gating pulse. In the special case $\xi = 1$, the scheme is coincident to the NOG scheme in which two driving pulses are identical.

The most appropriate way to relax the gating pulse duration demand while maintain the advantage of our scheme is to extend the factor $T/2$ according to Eq. (2). This scheme is naturally more suitable for the main driving pulse with longer wavelength due to the larger cycle T. By combining the second harmonic with the main pulse that leads to only one attosecond burst per cycle, the gating width is increased by a factor of 2 and the depletion effect by the leading edge is suppressed, similar to the method of double optical gating [14]. The gating pulse can be extended to sub-4 fs or even longer by applying one or several of these approaches. As shown in Fig. 3(b), IAP can be achieved even with a 3.5 fs gating pulse by employing a 1300 nm wavelength fundamental pulse with its second harmonics. By stretching the spectrum of a Ti:sapphire laser in a gas-filled hollow fiber and compressing the dispersion by a chirped mirror, generation of sub-4 fs laser pulses is already a routine in many laboratories [28].

The phase or time delay variation of the driving pulses results in the shift of the high harmonics emission time and the rotation of the synthesize wave front. Consequently, the temporal and spatial properties of the selected IAP vary with CEP. It indicates that CEP and time delay stability of the driving pulses is necessary to ensure the reproducibility for a long term experiment, while at the same time it implies that the flexibility of manipulating the number and relative intensity of the selected attosecond pulses by controlling CEP or time delay.

IV. CONCLUSION

In conclusion, we have proposed a gating method for IAP selection from APT based on the noncollinear geometry and WFR technique. By combining an intense main driving pulse and a noncollinear subcycle gating pulse to synthesize a tilted wave front only in the overlapping region, the selected attosecond pulse spatially separated from the fundamental beam, hence other attosecond pulses. The approach is studied by an analytical model and numerical simulations. Our method sets no restriction on the duration of the main driving pulse. Therefore, it is ideal for the generation of high-flux IAP by using an intense multicycle driving laser. The duration limit of the gating pulse can be relaxed by employing a long wavelength main driving pulse or combining with the two-color gating technique. Without any limitation to the duration of the main driving pulse, this scheme can also be used for the IAP generation from a dense plasma using a solid target where the high-energy laser pulse is critical [29].

ACKNOWLEDGMENTS

This work was partly supported by the National Key Basic Research Program of China (Grants No. 2013CB922401 and No. 2013CB922402), National Key Scientific Instrument and Equipment Development Projects (Grant No. 2012YQ12004704), National Natural Science Foundation of China (Grants No. 11374356 and No. 11474002), the International Joint Research Program of National Natural Science Foundation of China (Grant No. 61210017), and the State Key Program of National Natural Science of China (Grant No. 11434016).

[1] M. Hentschel, R. Kienberger, C. Spielmann, G. A. Reider, N. Milosevic, T. Brabec, P. Corkum, U. Heinzmann, M. Drescher, and F. Krausz, Nature (London) **414**, 509 (2001).

[2] J. Itatani, F. Quéré, G. L. Yudin, M. Y. Ivanov, F. Krausz, and P. B. Corkum, Phys. Rev. Lett. **88**, 173903 (2002).

[3] M. Uiberacker, T. Uphues, M. Schultze, A. J. Verhoef, V. Yakovlev, M. F. Kling, J. Rauschenberger, N. M. Kabachnik, H. Schröder, M. Lezius *et al.*, Nature (London) **446**, 627 (2007).
[4] J. Itatani, J. Levesque, D. Zeidler, H. Niikura, H. Pépin, J.-C. Kieffer, P. B. Corkum, and D. M. Villeneuve, Nature (London) **432**, 867 (2004).
[5] A. Schiffrin, T. Paasch-Colberg, N. Karpowicz, V. Apalkov, D. Gerster, S. Mühlbrandt, M. Korbman, J. Reichert, M. Schultze, S. Holzner *et al.*, Nature (London) **493**, 70 (2013).
[6] M. Schultze, E. M. Bothschafter, A. Sommer, S. Holzner, W. Schweinberger, M. Fiess, M. Hofstetter, R. Kienberger, V. Apalkov, V. S. Yakovlev *et al.*, Nature (London) **493**, 75 (2013).
[7] S. R. Leone, C. W. McCurdy, J. Burgdörfer, L. S. Cederbaum, Z. Chang, N. Dudovich, J. Feist, C. H. Greene, M. Ivanov, R. Kienberger *et al.*, Nat. Photon. **8**, 162 (2014).
[8] E. Takahashi, Y. Nabekawa, and K. Midorikawa, Opt. Lett. **27**, 1920 (2002).
[9] E. J. Takahashi, P. Lan, O. D. Mücke, Y. Nabekawa, and K. Midorikawa, Nat. Commun. **4**, 2691 (2013).
[10] Y. Wu, E. Cunningham, H. Zang, J. Li, M. Chini, X. Wang, Y. Wang, K. Zhao, and Z. Chang, Appl. Phys. Lett. **102**, 201104 (2013).
[11] E. Goulielmakis, M. Schultze, M. Hofstetter, V. S. Yakovlev, J. Gagnon, M. Uiberacker, A. L. Aquila, E. M. Gullikson, D. T. Attwood, R. Kienberger, F. Krausz, and U. Kleineberg, Science **320**, 1614 (2008).
[12] G. Sansone, E. Benedetti, F. Calegari, C. Vozzi, L. Avaldi, R. Flammini, L. Poletto, P. Villoresi, C. Altucci, R. Velotta, S. Stagira, S. De Silvestri, and M. Nisoli, Science **314**, 443 (2006).
[13] M. J. Abel, T. Pfeifer, P. M. Nagel, W. Boutu, M. J. Bell, C. P. Steiner, D. M. Neumark, and S. R. Leone, Chem. Phys. **366**, 9 (2009).
[14] H. Mashiko, S. Gilbertson, C. Li, S. D. Khan, M. M. Shakya, E. Moon, and Z. Chang, Phys. Rev. Lett. **100**, 103906 (2008).
[15] X. Feng, S. Gilbertson, H. Mashiko, H. Wang, S. D. Khan, M. Chini, Y. Wu, K. Zhao, and Z. Chang, Phys. Rev. Lett. **103**, 183901 (2009).
[16] H. Vincenti and F. Quéré, Phys. Rev. Lett. **108**, 113904 (2012).
[17] J. A. Wheeler, A. Borot, S. Monchoce, H. Vincenti, A. Ricci, A. Malvache, R. Lopez-Martens, and F. Quere, Nat. Photon. **6**, 829 (2012).
[18] C. M. Heyl, S. N. Bengtsson, S. Carlstrm, J. Mauritsson, C. L. Arnold, and A. L'Huillier, New J. Phys. **16**, 052001 (2014).
[19] M. Louisy, C. L. Arnold, M. Miranda, E. W. Larsen, S. N. Bengtsson, D. Kroon, M. Kotur, D. Guénot, L. Rading, P. Rudawski, F. Brizuela, F. Campi, B. Kim, A. Jarnac, A. Houard, J. Mauritsson, P. Johnsson, A. L'Huillier, and C. M. Heyl, Optica **2**, 563 (2015).
[20] J. B. Bertrand, H. J. Wörner, H.-C. Bandulet, E. Bisson, M. Spanner, J.-C. Kieffer, D. M. Villeneuve, and P. B. Corkum, Phys. Rev. Lett. **106**, 023001 (2011).
[21] K. T. Kim, C. Zhang, A. D. Shiner, S. E. Kirkwood, E. Frumker, G. Gariepy, A. Naumov, D. Villeneuve, and P. Corkum, Nat. Phys. **9**, 159 (2013).
[22] X. He, M. Miranda, J. Schwenke, O. Guilbaud, T. Ruchon, C. Heyl, E. Georgadiou, R. Rakowski, A. Persson, M. B. Gaarde, and A. L'Huillier, Phys. Rev. A **79**, 063829 (2009).
[23] K. V., Y. Mairesse, B. Carr, M. B. Gaarde, P. Johnsson, S. Kazamias, R. Lopez-Martens, J. Mauritsson, K. J. Schafer, P. Balcou, A. L'Huillier, and P. Salires, J. Mod. Opt. **52**, 379 (2005).
[24] M. T. Hassan, A. Wirth, I. Grgura, A. Moulet, T. T. Luu, J. Gagnon, V. Pervak, and E. Goulielmakis, Rev. Sci. Instrum. **83**, 111301 (2012).
[25] H. Muller, Appl. Phys. B **74**, s17 (2002).
[26] M. Lewenstein, P. Balcou, M. Y. Ivanov, A. L'Huillier, and P. B. Corkum, Phys. Rev. A **49**, 2117 (1994).
[27] C. M. Heyl, P. Rudawski, F. Brizuela, S. N. Bengtsson, J. Mauritsson, and A. L'Huillier, Phys. Rev. Lett. **112**, 143902 (2014).
[28] H. Teng, C.-X. Yun, X.-K. He, W. Zhang, L.-F. Wang, M.-J. Zhan, B. bing Wang, and Z.-Y. Wei, Opt. Express **19**, 17408 (2011).
[29] C. Thaury and F. Quéré, J. Phys. B: At. Mol. Opt. Phys. **43**, 213001 (2010).